Physical Vapor Transport of lead telluride

W. Palosz*

NASA-Marshall Space Flight Center, Huntsville, Alabama 35812, USA

Ph. (256) 544-1272, fax. (256) 544-6762 , e-mail: witold.palosz@msfc.nasa.gov

PACS 81.05.Hd, 81.10.Bk, 81.20.Ym

Keywords: PbTe, PVT, residual gas

Abstract

Mass transport properties of physical vapor transport of PbTe are investigated. Thermochemical analysis of the system and its implications for the growth conditions are discussed. The effect of the material preparation and pre-processing on the stoichiometry and residual gas pressure and composition, and on related mass flux is shown. A procedure leading to high mass transport rates is presented.

1. Introduction

Lead chalcogenide compounds and alloys are narrow-gap semiconductors with applications in devices like lasers and detectors, particularly in the infrared spectral range [1 - 4]. The unique properties of lead salt diode lasers are: wide wavelength operating range, high mobilities, good thermoelectric properties, tunability, narrow line width, and high local and temporal resolution [5]. Other advantages of these materials are: good homogeneity, rather low price, and easier manufacturing processes relative to HgTe-based materials. Bulk crystals of these materials are used mostly as substrates for manufacturing different devices, primarily tunable diode lasers operable in the mid-infrared region from 3 to 30 microns and room temperature IR detectors operating in the range 2 – 4.5 micrometer. While the market of IR detectors has recently been dominated by HgTe-based materials, Pb-chalcogenides have still important applications in devices like diode lasers for molecular spectroscopy and gas monitors [5], and may become a key device material for IR integrated optics and telecommunication systems [6, 7]. Use of appropriate ternary alloys enables tuning the bandgap to a desired wavelength and/or tailoring the lattice constant for matching the substrate and the active epilayer lattice constant. For example, (Pb, Sn)Te is a widely used IV-VI ternary material allowing for an adjustment of the spectral range of the device by an appropriate selection of SnTe content

---

* *Universities Space Research Association staff scientist*

in the crystal [5]. Different IV-VI substrates can be used for low dimensional magnetic structures and applications of semimagnetic semiconductors (e.g. EuTe-PbTe [8 - 10) and applications requiring good thermoelectric properties of the material [11 – 14]. Easy tuneability by temperature/current and narrow line width make the materials particularly useful in high-resolution spectroscopy and gas monitoring devices [2].

Best quality crystals of IV-VI compounds are being grown from the vapor phase by physical vapor transport (PVT). A number of papers have been published on growth of these materials by this technique (i.e. [15 - 23]). However, except for a few papers ([20] - PbTe, [21, 23] - PbSnTe) no more detailed analysis of the process has been presented. In this paper we investigate, theoretically and experimentally, physical vapor transport of the most widely used IV-VI material, PbTe.

The two key factors determining mass transport properties in PVT systems are the stoichiometry/congruency of the vapor and the amount of inert gas in the system. We investigate in detail the effect of different procedures of the source material preparation and processing on these two factors. Our experimental mass transport rates are compared with those predicted theoretically.

2. *Theoretical calculations*

Lead telluride vaporizes according to the reactions

$$PbTe(c) = PbTe(g), \qquad K1 = P_{PbTe}, \tag{1}$$

$$PbTe(c) = Pb(g) + 0.5Te_2(g), \qquad K2 = P_{Pb} P_{Te_2}^{0.5}, \tag{2}$$

$$Te_2(g) = 2\,Te(g), \qquad K3 = P_{Te}^2 / P_{Te_2}, \tag{3}$$

where 'c' and 'g' denote a condensed and gaseous phase, respectively. With sufficient deviation from stoichiometry a second, Pb-rich or Te-rich liquid phase forms and the partial pressure of the related element is determined by corresponding redactions

$$Pb_{PbTe}(l) = Pb(g), \qquad P_{Pb} = a_{Pb}\, P_{Pb}^{o}, \tag{4}$$

$$2\,Te_{PbTe}(l) = Te_2(g), \qquad P_{Te_2} = a_{Te}^2 P_{Te_2}^{o}, \tag{5}$$

where $Pb_{PbTe}(l)$ and $Te_{PbTe}(l)$ are PbTe-saturated Pb and Te liquid phases, respectively, P°'s are saturated vapor pressures over pure phases, and a's are activities of the respective elements.

Assuming diffusion limited conditions, the overall mass transport in one-dimensional approximation can be described by a set of Maxwell transport equations of the form [24]

$$-(1/RT)(dP_i/dl) = (J_i P_j - J_j P_i) / D_{ij}, \qquad i, j = PbTe, Pb, Te_2, Te, Z. \tag{6}$$

In these equations, J's are the mass fluxes (in mole cm^{-2} s^{-1}) and P's are the partial pressures of respective species, D_{ij}'s are binary diffusion coefficients, T is the temperature, l is the coordinate along the diffusion path, Z is the inert

component(s) of the vapor phase (see below), and R is the gas constant. Uniform total pressure, P_t , throughout the ampoule and no net transport of the inert gas yield

$$Pt = P_{PbTe}(0) + P_{Pb}(0) + P_{Te_2}(0) + P_{Te}(0) + P_Z(0) =$$

$$P_{PbTe}(L) + P_{Pb}(L) + P_{Te_2}(L) + P_{Te}(L) + P_Z(L) = \text{constant}, \qquad (7)$$

$$J_Z = 0. \qquad (8)$$

From the set of equations (1 - 3) and, when applicable, eq. (4) or (5), the equilibrium partial pressures were calculated for stoichiometric and 2-phase (solid+liquid) conditions. The mass flux was computed from eqs. 6 – 8, the equilibrium constants (eqs. 1 – 3), partial pressures over the liquid phase (eqs. 4 or 5, if applicable), and a given amount of inert gas in the system.

The equilibrium partial pressures for reactions (1 - 3) were computed from the dependence of the equilibrium constants K on the change of the Gibbs function, G =- R T lnK, using thermochemical data given in refs. [25 - 27]. The pressures over pure liquid lead and tellurium phases were taken from refs. [27, 28]. In lieu of accurate literature data near the melting point (particularly on the Pb-rich side of the P-T phase diagram), the equilibrium partial pressures were calculated as follows. The partial pressures over PbTe-saturated Pb/Te phase were calculated from eq. 4/5. The activities of Pb and Te in the liquid phases were obtained from

$$a_i = X_i f_i = X_i \exp(-\alpha (1-X_i)/RT), \qquad i = Pb, Te \qquad (9)$$

where X_i is the mole fraction of the atomic specie (Pb/Te), f_i is its activity in the liquid phase, and α is the exchange energy factor [29]. The values of X_i and α were calculated based on the regular associated solution model [30] using the procedure developed by Szapiro [31]. To calculate the $X_i(T)$ and α parameter, X-T diagram of Pb-Te system given in ref. [32] was used.

The binary diffusion coefficients used in the mass transport calculations were computed from molecular constants [33] using the procedures described in ref. [34].

3. *Experimental procedures*

The source material was synthetized from high purity (m6N) lead and tellurium elements. Stoichiometric amounts of Pb and Te (total of up to 400g) were loaded into silica glass ampoules, evacuated, then sealed with 0.1 atm of hydrogen. (The addition of hydrogen removes at least some of the oxide impurities and prevents etching/sticking of the material to the ampoule wall.) The mixture was gradually heated up to 900 – 950°C for about 4 days. The synthetized material was ground and sifted (mesh 80) before further use.

The mass transport experiments were performed in sealed silica glass ampoules of 10 mm inner diameter and 20 – 25 cm in length. The ampoules were cleaned and outgassed under high vacuum at 1000°C for 16 hours. Under such conditions the amount of gas released from silica during the subsequent material processing is low relative to that generated by the source and can be ignored [35]. About n = 0.05 mole of PbTe (such as to obtain the n/V_f ratio, where V_f is the free volume in the ampoule, of 3 mmole/cm^3) was loaded into the ampoule with or without (as

needed) a 20 – 30 mg of elemental Pb, and connected to high vacuum. In a few cases other amounts of the source were used. After evacuating to 10^{-5} Torr or better the ampoule was backfilled (when desired) with 0.5 atm of H_2 and baked at 600°C for 20 min followed by a 20 min bakeout under dynamic vacuum, then cooled. Two series of experiments were performed. In the first series, after the initial bakeout the ampoule was just sealed off. In the second series, two consecutive residual gas generating annealings were done as follows. Initially, after the bakeout, the ampoule was sealed with a plug furnished with a fine tip pointing toward the vacuum system. In some cases, the initial baking was done when the ampoule was connected to the vacuum through a 4 cm long, 1 mm ID capillary, and lasted for 2 hours at 800 or 850°C prior to sealing. The capillary allowed for a bakeout under dynamic vacuum without an excessive loss of the source from the ampoule. The sealed ampoule was annealed at 850°C for 1 or 48 hours (annealing A1), then the amount of gas (P1) was measured by breaking the plug tip and releasing the residuals to the measuring chamber. After the measurement the ampoule was evacuated and sealed again.

Prior to the mass flux runs, the source was sintered at 700°C under small reverse temperature gradient for 1 hour, then equilibrating isothermally (without transport) for 1 h at the source temperature. For selected experiments of the second series, the actual mass transport was preceeded by a 48 h annealing (A2) at the growth temperature. In one case the source was melted (for 20 min) prior to run. The mass transport lasted for up to 35 hours in the first series, and up to 5 h in the second, during which up to 20% of the source was transported. For the sake of internal consistency, the same batch of the source material was used for all experiments of a given series. The amount (P2) and composition of the gas formed in the ampoules was measured using the technique described earlier [35]. For the sake of further analysis, the actually measured pressures were recalculated into the equivalent effective pressures of carbon monoxide using the formula

$$Pz = P_{CO} + P_{CO_2}(D_{CO\text{-}PbTe}/D_{CO_2\text{-}PbTe}) + P_{H_2}(D_{CO\text{-}PbTe}/D_{H_2\text{-}PbTe}) + P_{H_2O}(D_{CO\text{-}PbTe}/D_{H_2O\text{-}PbTe}), \quad (10)$$

where D's are the binary diffusion coefficients of respective pairs.

4. Results and discussion

Mass transport and crystal growth in PVT systems is normally limited by diffusion which depends on the partial pressures of the constituent and inert gas components of the vapor phase. Residual gases and non-congruent composition of the vapor (excess constituent element(s)) present in the vapor phase form a diffusive resistance to the mass flow and may seriously limit the practical usefulness of PVT techniques. Equilibrium partial pressures and their effect on the growth conditions are discussed in section 4.1. The issue of residual gases in our system is discussed in sections 4.2 and 4.3.

4.1 Equilibrium partial pressures

The results of our equilibrium partial pressures calculations are shown in Fig. 1. As can be seen, dissociation of PbTe (eq. 2) is very small (less than 1% below about 870°C), so gaseous mass transport of lead telluride occurs essentially by PbTe molecules. In general, volatility of some excess constituent elements (Pb and Te) may contribute to mass transport conditions in the system. Volatility of Pb over pure Pb(l) phase is relatively low, and

even lower in the presence of PbTe, being at least 1 order of magnitude below that of PbTe (in the temperature range of our interest. i.e. > 750°C). Moreover, a significant accumulation of excess Pb (by the 'sweeping' effect of the transporting constituent species, [36]) at the crystal-vapor interface and corresponding reduction in the mass transport rate will be limited by precipitation of Pb(l) phase. As a result, the effect of Pb(l) on mass transport conditions is low and may be significant only at low residual gas pressures (less than about 0.5 Torr, c.f. Fig. 4). The volatility of tellurium is much higher, and its pressure may exceed that of PbTe by one order of magnitude or more (Fig. 1). Therefore, a large amount of excess tellurium can remain in the vapor phase and significantly reduce the growth rate. Such excess of tellurium can be prevented by adding to the source a sufficient amount of elemental Pb which would serve as a tellurium getter without contributing a noticeable amount of extra Pb atoms to the vapor (what has already been recognized earlier [16]). Above about 860°C the gettering effect becomes limited due to the Pb-saturation line crossing the Pb-rich, Te_2(min) homogeneity range of PbTe; above this point even originally stoichiometric source will decompose to produce the minimum partial pressure of tellurium and corresponding amount of PbTe-saturated liquid Pb phase. Above about 830 – 860°C the effect of excess Pb or Te_2 species accumulated in the deposition zone becomes more and more pronounced and leads to a reduction in mass transport rate in the system (c.f. Fig. 4).

A presence of liquid Pb in the source may lead to precipitation of lead in the crystallization zone. That happens when the transport rate of lead to the cold zone exceeds that of tellurium and of the solubility limit of Pb in PbTe (about 10^{-4} at 800°C [32]. Fig. 2 shows the relative rate of Pb precipitation as a function of the source temperature for two values of undercooling and three levels of residual gas pressure in the system. The onset of Pb precipitation for low undercooling (10°C) occurs about 808°C, and goes up with increasing undercooling to 826°C at $\Delta T = 50$°C. The rate of precipitation incrases with increasing the amount of residual gas in the system, and may exceed 1 % at lower temperatures and higher P_z levels.

4.2 The effect of the source grain size, annealing in hydrogen, and presence of Pb(l)

The results of our first series of experiments in terms of the amount and composition of residual gas and mass flux are given in Table 1a. For the sake of clarity, only the major components of the residual gas are shown. As can be seen, baking the source without hydrogen has apparently a limited effect on removal of oxygen (oxides) from the source, and the residual gas formed after such treatment is dominated by carbon dioxide (exp. 1, 2, 11, 13). Exposing the source to air for one week apparently increases the amount of oxygen and corresponding CO_2 content, particularly when finely ground source is used and no baking in hydrogen is applied (exp. 13). Signs of etching of silica (reaction with PbO) are usually observed in ampoules prepared without H_2. Baking in hydrogen reduces the amount of oxygen, but the total pressure remains often similar to those found in related ampoules baked without hydrogen, with a portion of the gas being H_2 (exps. 12, 14, 21).

When coarse source material is used, a moderate (about 0.5 Torr) amount of residual gas forms under our experimental conditions (exps. 1 - 3). However, the mass flux in ampoule #1 is two orders of magnitude less than those in the other two experiments (2 and 3). Apparently, the low mass flux in exp. 1 was caused by a presence, in

the original source material, of excess Te which was not removed during the material pre-treatment due, primarily, to the large size of the grains. When similar processing conditions but finely ground source was used, the mass flux was higher by over one order of magnitude even without addition of excess Pb and despite three times higher residual gas pressure in the ampoule (exp. 11). A build-up of excessive pressure of Te was prevented in exps. 2 and 3 by the presence of liquid Pb in the system, thus the mass flux in these experiments was considerably increased relative to that in exp. 1.

Using finely ground source facilitates removal of excess Te, but generates larger amounts of residual gas (and correspondingly lower mass flux) than coarse materials, where part of the impurities remain trapped inside grains (compare exps. 2, 3, 11, and 12). Higher temperature of the source pre-treatment reduces the amount of residual gas and increases the mass transport rate (exp. 21 and 22). Exposing the source material to oxygen (air) in room temperature leads to surface oxidation. It is particularly relevant in case of powdered materials and may lead to an increase in residual gas pressure particularly if annealing in hydrogen is not applied (exp. 13).

4.3 Intermediate removal of residual gas

The results of the second series of our material preparation experiments are shown in Table 1b. In the reference experiment, R, after our regular ampoule preparation procedure only one annealing without residual gas removal was performed. That resulted in a moderate growth rate occurring under relatively large amount of residual gas (mostly CO) conditions. In the remaining experiments two consecutive annealings and residual gas measurements were made. As follows from Table 1b, after the initial annealing (A1) the amount of gas generated in the ampoule is typically about 0.5 Torr (at RT). Extended (A1 = 48h, exp. d) annealing prior to the gas removal has a relatively small effect on the initial amount of residuals (P1), but a much stronger effect on lowering the final pressure (P2) and corresponding increase in mass flux. That suggests, that after the long A1 annealing considerably larger amount of CO was generated/released from the source than after 1 h annealings. It reduced the final amount of gas and increased the mass transport rate (compare exps. c and d). Without annealing prior to the growth process (A2) the generation of residual gases is apparently reduced and their effective amount present during the growth process is lower resulting in higher growth rate (compare exps. a and c).

Purification of the source by annealing under semi-closed conditions is an effective way of reducing the amount of residual gases in the system. Such purification performed at 800°C (exp. e) reduced the amount of gas generated during the subsequent (A1) ampoule annealing by a factor of 5. However, apparently too low purification and annealing temperature led to a relatively large portion of the impurities remaining in the source, resulting in a substantial amount of residual gas formed during the second part of the process and in lower growth rate relative to some other experiments. Purification of the source at 850°C with a long subsequent annealing led to a very low amount of gas and very high mass transport rate even without excess Pb in the source (exp. f). Purification of the source under semi-closed conditions has the additional advantage of adjusting the composition of the source (removal of excess elements) occurring under most desired, nearly equilibrium conditions.

Melting of the source prior to growth apparently generated an additional amount of gas (exp. m). Also, the amount of elemental tellurium in the vapor over the source apparently increased (as indicated by the observed change in the color of the vapor) and, combined with the higher residual gas pressure, led to a much lower growth rate than in the other experiments of the series. Obviously, melting of the source leads to a noticeable decomposition of lead telluride (Fig. 1) which does not revert completely to the initial stoichiometric conditions upon solidification due to low diffusivities and long diffusion distances in the solidified bulk material.

4.4 The effect of the source amount, temperature, and growth time

Theoretically calculated and experimentally obtained dependence of mass flux on residual gas pressure in the system is shown in Fig. 3. As might be expected, the amounts of the gas formed in the ampoules and the related mass fluxes are strongly dependent on the amount (visualized by the size of the open circles in Fig. 3) of the source in the ampoule. The lowest pressure and highest flux was obtained for the experiment with n/V_f ratio of 0.6 mmole per cm^3, and the opposite was found for the one with n/V_f of 11 mmole/cm^3. Intermediate values were found for the standard conditions of 3 mmole/cm^3 (Fig. 3). Steady-state mass transport is established quite fast, as indicated by the results obtained for similiarly prepared experiments but conducted for 1 and 24 hours (open triangles and open circle, respectively). Some effect of the processing time on the residual gas pressure was observed when the procedure discussed in section 4.3 was applied and the amount of residual impurities was reduced. Under our experimental conditions, the results obtained with apparently stoichiometric material are close to those obtained with initial addition of lead to the source (solid triangles). Since our basic experiments were prepared without intentional addition of a constituent element, the good agreement between the experimental and predicted results indicates that our experimental procedure leads to close to stoichiometric composition of the source.

For comparison, extreme exprimental results of our mass transport experiments are shown in Fig. 3 too. In the experiment represented by the open square, the source was pre-purified under poor vacuum conditions (about 1 mTorr). The resulting contamination (due to source oxidation) was apparently not removed during our standard material pre-processing conditions (c.f. section 3) and high residual gas pressure (CO_2 and H_2O) and very low mass flux resulted. On the other extreme, using our most effective procedure (c.f. section 4.3), very low residual gas pressure and very high mass transport rate (2 orders of magnitude higher than those obtained using our standard ampoule preparation procedure) was achieved (solid square in Fig. 3).

Fig. 4 shows the experimental and theoretical results on the dependence of mass flux on the source temperature in the presence of a liquid Pb phase. Our experimental results (full circles) are, on average, about 2 times lower than those predicted theoretically for the same amount of residual gas as those found in thye experimental ampoules (about 1.5 Torr of "CO"), which is within the combined uncertainty of the thermochemical data used in the theoretical calculations and of the experimental measurements. At the highest temperature (900°C), the experimental results are higher than expected. As discussed in section 4.1, at T(source) > 830 – 860°C the diffusive mass transport rate may be expected to deviate from that predicted for congruent mass transport conditions (dashed line in Fig. 4) due to the presence of Pb(l) phase and decomposition of PbTe at higher temperatures. Deviation from

congruent mass transport conditions is also caused by dissociation of PbTe combined with unmatched diffusivities of the resulting Pb, Te, and Te_2 species. Apparently, the Pb-rich homogeneity range is at a higher temperature range than that calculated in this work from the available literature data. This discrepancy is not surprising, given the fact that there is a considerable scatter of experimental data on the liquidus of PbTe, particularly on the Pb-rich side, and the commonly assumed X-T diagram of the system is a relatively arbitrary choice particularly in the range close to the melting point (which is the region relevant for our analysis).

5. *Summary and conclusions*

A good control of mass transport and crystal growth conditions in PVT of lead telluride requires an appropriate adjustment of the stoichiometry of the vapor and of the amount of residual gas in the system. Mass transport rate may be significantly reduced by a presence of excess tellurium, but relatively little by excess of Pb in the source. At source temperatures near the melting point the transport may be reduced even if stoichiometric source is used. Baking the source under vacuum allows for a good adjustment of the source stoichiometry if finely ground material is used. Alternatively, a build up of excess tellurium pressure can be prevented by (small) addition of Pb to the source. Such technique may also lead to a better reproducibility of mass transport conditions in the system. It may, however, lead to a formation of liquid Pb in the deposition zone and to a presence of Pb-inclusions in the crystals grown at lower temperatures.

The pressure of residual gas generated in the system depends strongly on the ratio of the amount of the source to the free volume in the ampoule. With our standard n/V_f ratio of 3 mmole/cm^3 and a simple, 15 - 20 min bake-out of the finely powdered source under vacuum, the pressure of residual gas formed is typically in the range 1 – 3 Torr. The amount of the gas can be substantially reduced using our special procedure of intermediate annealing and gas removal, particularly when combined with an extended bake-out under semi-closed conditions. With a proper material preparation procedure, reasonable (and even high) crystal growth rates can be achieved even at relatively low temperatures, small undercoolings, and long diffusion paths between the source and the crystal.

The results of our more extended studies on generation of residual gas from different source materials will be presented in a separate publication [37].

Acknowledgments

The support of this work by the Microgravity Science and Applications Division of the National Aeronautics and Space Administration is gratefully acknowledged.

References

1. Semiconductors and Semimetals, vol. 5, ed. R. K. Willardson and A. C. Bear (Academic Press, 1970).
2. H. Preier, Semicond. Sci. Technol. 5 (1990) S12.
3. M. Tacke, Infrared Phys. Tech. 36 (1995) 447.
4. Z. Feit, M. McDonald, R. J. Woods, V. Archambault, and P. Mak, Appl. Phys. Lett. 68 (1996) 738.
5. H. Preier, Semicond. Sci. Technol. 5 (1990) S12.
6. M. Tacke, B. Spanger, A. Lambrecht, P. P. Norton, and H. Bottner, Appl. Phys. Lett. 53 (1988) 2260.
7. B. Spanger, U. Schiessl, A. Lambrecht, H. Bottner, and M. Tacke, Appl. Phys. Lett. 53 (1988) 2582.
8. L. Bergomi and J. J. Chen, Phys. Rev. B 56 (1997) 3281.
9. J. Blinowski and P. Kacman, Acta Phys. Pol. A 92 (1997) 719.
10. A. Stachow-Wojcik, A. Twardowski, T. Story, W. Dobrowolski, E. Grodzicka, and A. Sipatov, Acta Phys. Pol. A 92 (1997) 985.
11. L. D. Hicks and M. S. Dresselhaus, Phys. Rev. B 47 (1993) 12727.
12. L. D. Hicks, T. C. Harman, X. Sun, and M. S. Dresselhaus, Phys. Rev. B 53 (1996) R10493.
13. G. D. Maham, Solid State Physics, vol. 51 (Academic Press, New York 1998), p. 81.
14. G. D. Mahan, B. Sales, and J. Sharp, Phys. Today 50 (1997) 42.
15. S. G. Parker, J. E. Pinelli, and R. E. Johnson, J. Elect. Mater. 3 (1974) 731.
16. T. C. Harman and J. P. McVittie, J. Electr. Mat. 3 (1974) 843.
17. H. Maier, D. R. Daniel, and H. Preier, J. Crystal Growth 35 (1976) 121.
18. N. Tamari and H. Shtrikman, J. Crystal Growth 43 (1978) 378.
19. Z. Golacki, Z. Furmanik, M Gorska, A. Szczerbakow, and W. Zahorowski, J. Crystal Growth 60 (1982)
20. J. Zoutendyk and W. Akutagawa, J. Crystal Growth 56 (1982) 245.
21. T. V. Saunina, D. B. Chesnokova, and D. A. Jaskov, J. Crystal Growth 71 (1985) 75.
22. Z. Golacki, M. Gorska, T. Warminski, and A. Szczerbakow, J. Crystal Growth 74 (1986) 129.
23. M. Fabbri, I. N. Bandeira, and L. C. M. Miranda, J. Crystal Growth 104 (1990) 435.
24. H. L. Toor, A. I. Ch. E. Journal 3 (1957) 198.
25. I. Barin and O. Knacke, Thermochemical Properties of Inorganic Substances (Springer, Berlin 1974.
26. I. Barin, O. Knacke, and I. Kubaschewski, Thermochemical Properties of Inorganic Substances, Supplement (Springer, Berlin 1977).
27. R.F.Brebrick and A.J.Strauss, J. Chem. Phys. 40 (1964) 3230.
28. Selected Values of the Thermodynamic Properties of the Elements, Ed. R. Hultgren, (Am. Soc. for Metals, 1973).
29. E. A. Guggenheim, Mixtures (Oxford University Press, London, 1952).
30. A. S. Jordan, Met. Trans. 1 (1970) 239.
31. S. Szapiro, J. Electron. Mat. 5 (1976) 223.

32. N. Kh. Abrikosov, V. F. Bankina, L. V. Poretskaya, L. E. Shelimova, and E. V. Skudnova, Semiconducting II-VI, IV-V, and IV-VI Compounds (Plenum Press, NY 1969).

33. R. A. Svehla, NASA Technical Report R-132, 1962.

34. H. Wiedemeier, D. Chandra, and F. C. Klaessig, J. Crystal Growth 51 (1981) 345.

35. W. Palosz, J. Jpn. Soc. Microgravity Appl. 15 (Suppl. II) (1998), 454.

36. M. M. Faktor and I. Garrett, Growth of Crystals from the Vapour (Chapman and Hall, London, 1974).

37. Palosz et al., in preparation.

Figures

Fig. 1 Partial pressures in PbTe system as a function of temperature.

Fig. 2 Theoretically calculated deposition rate of elemental Pb during physial vapor transport of lead telluride as a function of the source temperature.

Fig. 3 Theoretical (solid line) and experimental results on the dependence of mass flux on the pressure of residual gas (carbon monoxide) in the system. Open triangles, 1h mass transport; full triangles, source with excess Pb; open square, heavily oxidized source; full square, experiment f, Table 2b.

Fig. 4 Theoretical and experimental results on the dependence of mass flux on the source temperature. Residual gas pressure for the experimental points (full circles) corresponds to 1.5 Torr of carbon monoxide. Theoretical curves: solid line, Pb(l) phase in the source region; dashed line, hypothetical congruent transport of all constituent species.

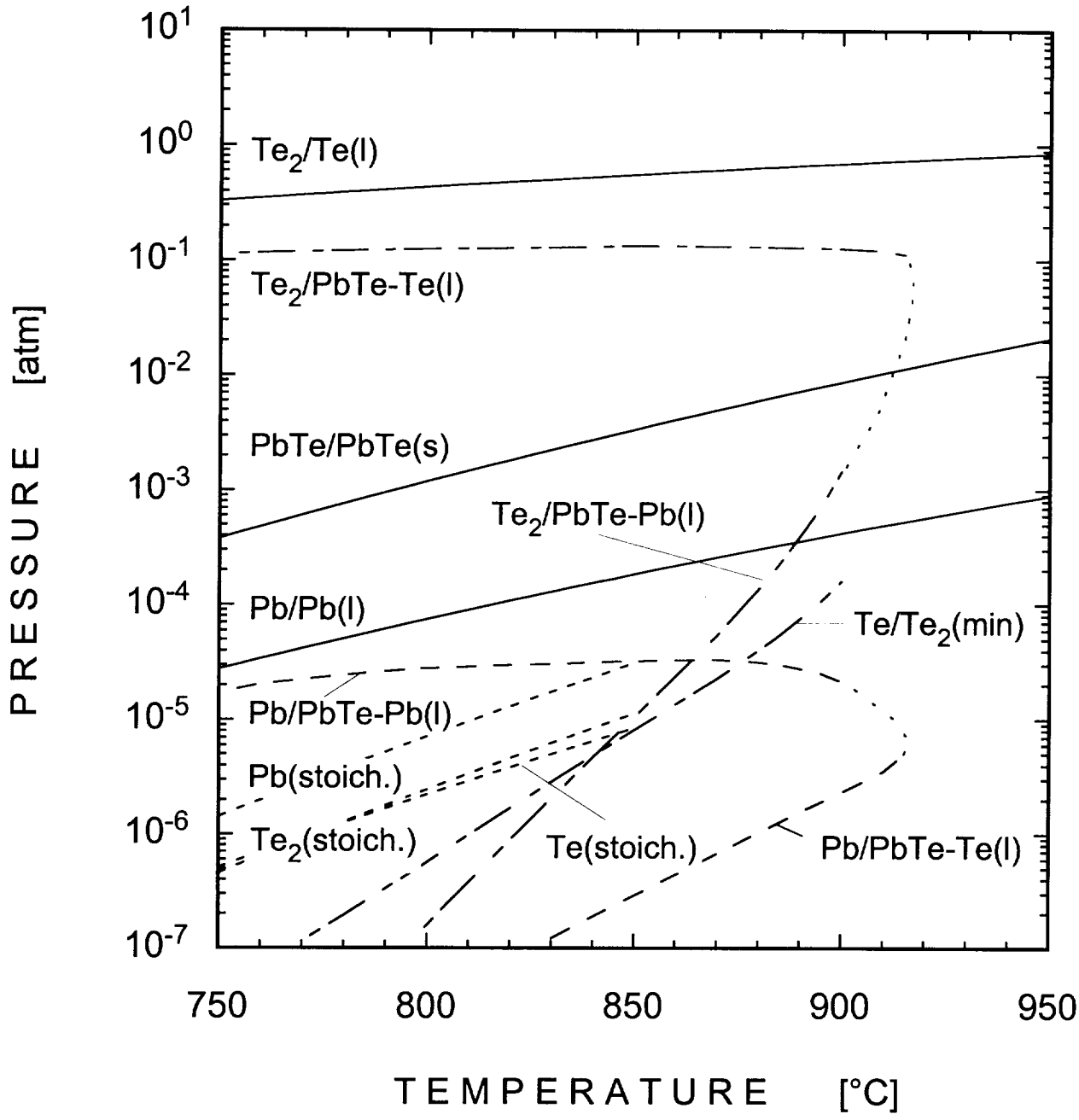

W. Palosz, "Physical Vapor Transport of Lead Telluride " *Fig. 1*

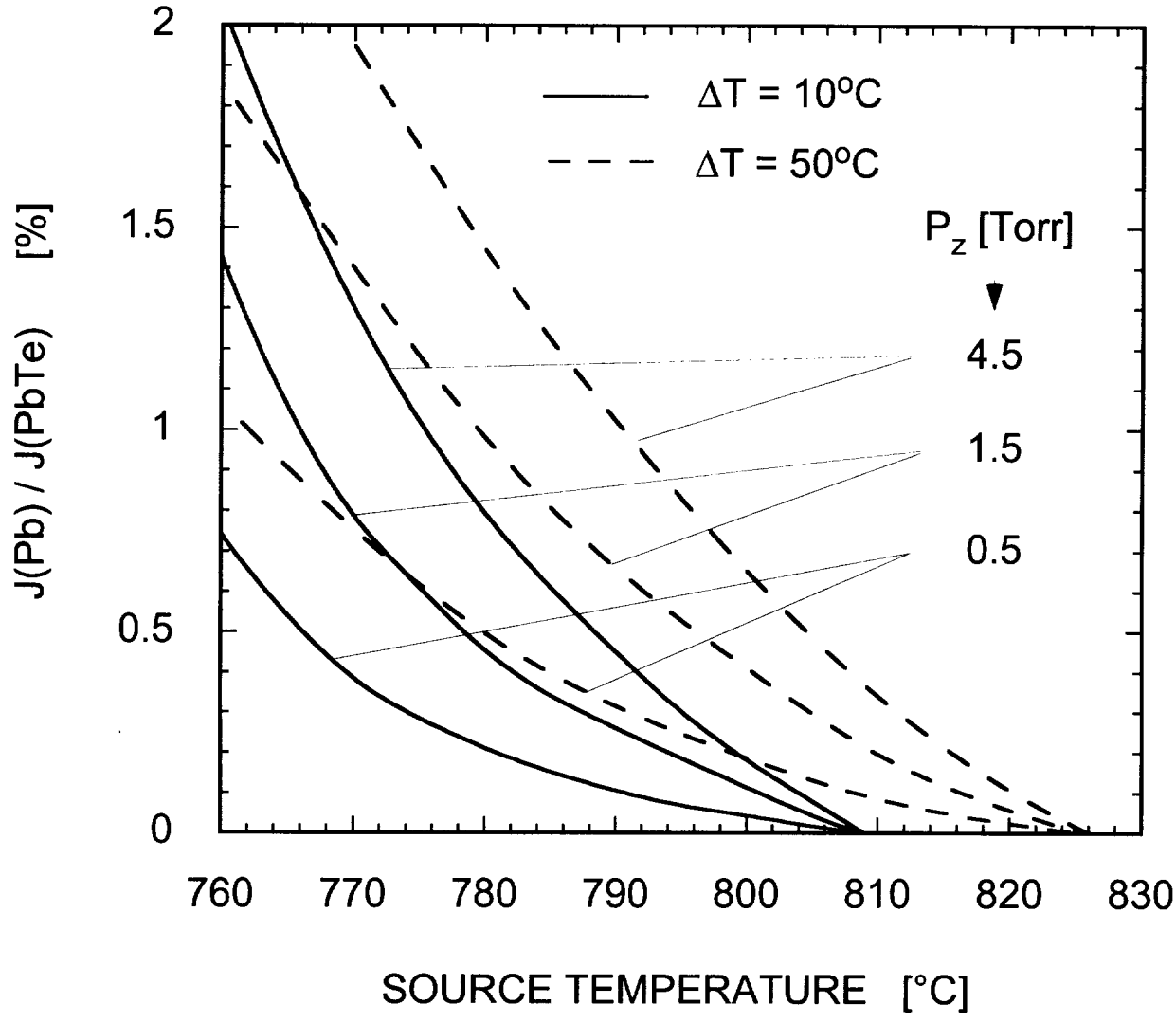

W. Palosz, "Physical Vapor Transport of Lead Telluride" *Fig. 2*

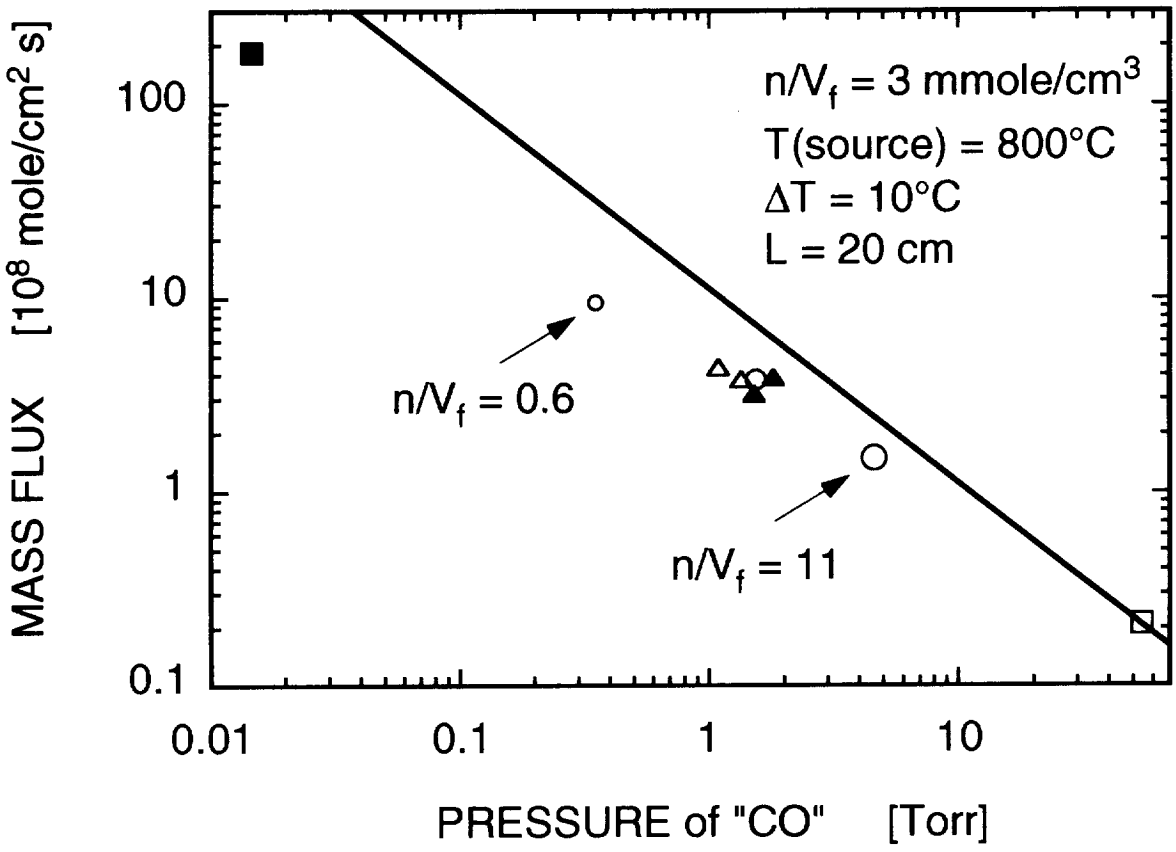

W. Palosz, "Physical Vapor Transport of Lead Telluride"

Fig. 3

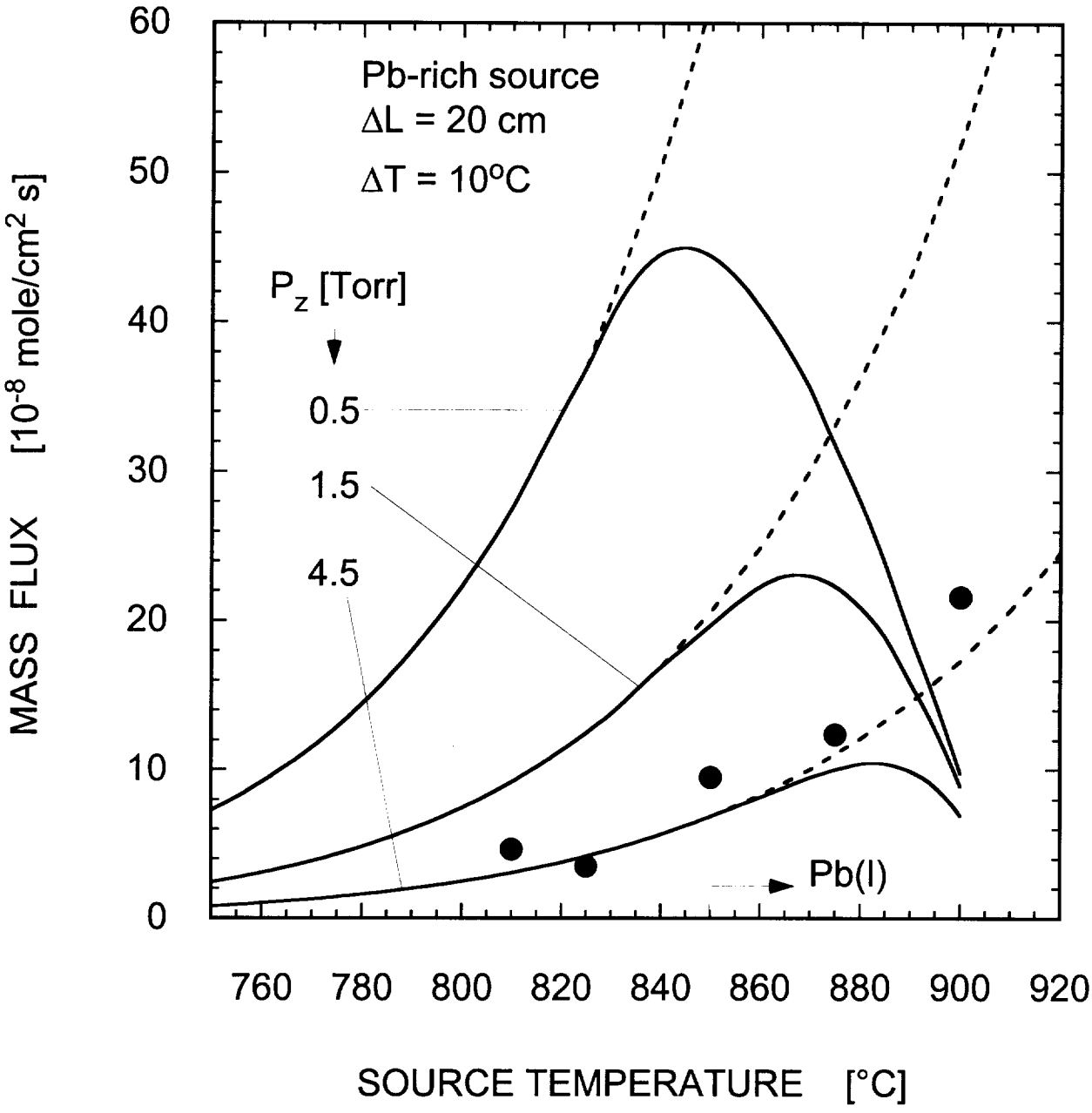

W. Palosz, "Physical Vapor Transport of Lead Telluride" *Fig. 4*

Table 1a. Mass flux and residual gas formed in mass transport ampoules. T(source) = 800 °C, ΔT = 10°C, L = 20 cm.

Run #	Grain size [mm]	H_2 annealing	Pb(*l*)	Flux·10^8 [mole/cm^2 s]	P [mTorr at RT]	P* [mTorr at RT]	Composition [%] H_2	CO	CO_2
1	1 - 3			0.14	82	120		10	80
2	1 – 3 (1)		yes	10.3	97	135			90
3	1 – 3	yes	yes	13.2	165	150	22	62	16
11	< 0.1			2.6	270	380			75 (2)
12	< 0.1	yes		3.8	420	430	13	62	22
13	< 0.1 (1)			1.2	900	1360			> 96
14	< 0.1 (1)	yes		2.4	810	730	33	26	35
21 (3)	< 0.1	yes	yes	9.1	470	380	18	74	7
22 (3)	< 0.1	yes	Yes(4)	28	180	150	20	72	28

(1) oxidized in air for 1 week

(2) + 25% H_2O

(3) T(source) = 850 °C

(4) annealing and baking at 700°C

Table 2b.

Run#	Pb(*l*)	Capil.	A1 [h]	P1 [mTorr at RT]	A2	P2 [mTorr at RT]	P* [mTorr at RT]	Flux10^8 [mole/cm^2 s]	Gas composition [%] H_2	CO
R	yes				yes	270	294	15	12	80
a	yes		1	500		36	25	83	40	45
b			1	490		27	16	75	50	35
c	yes		1	510	yes	66	47	47	35	55
d	yes		48	590	yes	21	11	95	58	35
e		yes (1)	1	100	yes	108	30	50	89	11
f		yes	48	480	yes	20	4	185	98	
m	yes		1	780	(2)	180	121	19	41	55

(1) baking and annealing at 800°C

(2) melting 1000°C/20 min